

Characterization of Ca–Bi–Mo Oxide Catalyst for Selective Propane Ammoxidation, Using XRD, XPS, TPRX/TPRO, and IR/Raman

Seong Ihl Woo,* Jong Seob Kim, and Hee Kwon Jun

Department of Chemical & Biomolecular Engineering and Center for Ultramicrochemical Process Systems, Korea Advanced Institute of Science and Technology, 373-1 Guseong-dong, Yuseong-gu Daejeon, 305-701, Republic of Korea

Received: January 13, 2004; In Final Form: April 23, 2004

The physicochemical properties of highly active and selective Ca–Bi–Mo oxide for ammoxidation of propane to acrylonitrile were investigated by XRD (powder), IR/Raman, XPS, and TPRX/TPRO (temperature programmed reaction/temperature programmed reoxidation) techniques. It was found that the phases in the Ca–Bi–Mo oxide varied with the composition of the oxide. The modified γ -bismuth molybdate (γ -Bi₂-MoO₆) and defective Ca–Bi–Mo phases produced by addition of Bi oxide played an important role in propane ammoxidation to acrylonitrile. XPS results revealed that the mole ratio of elements on the surface was different from that in the bulk. The concentration of bismuth decreased from the surface to the inner layer of Ca_xBi_{12-x}Mo₁₂ oxide, while the concentration of calcium increased from the surface to the inner layer. The Ca–Bi–Mo oxide showed good catalytic performance when an appropriate amount of calcium oxide was present on the surface along with Bi and Mo oxides. The addition of Ca oxide into Bi–Mo oxide decreased the number of active sites for complete oxidation and increased the ability of reoxidation (O₂ consumption) of reduced catalysts.

Introduction

Most industrial organic chemicals are made from petroleum or natural gas. About 25% of them are manufactured by the selective partial (amm)oxidation over heterogeneous catalysts which are mostly multicomponent mixed-metal oxide catalysts. The raw materials of the present partial oxidation and ammoxidation are mainly olefinic hydrocarbons. However, extensive studies have been performed to manufacture the required chemicals from paraffinic hydrocarbons. The most successful partial oxidation of alkanes is the production of maleic anhydride from *n*-butane over a VPO (vanadium phosphorus oxide)-based catalyst.¹ This is the only process used in the U.S.A. due to its low feed cost and reduced environmental pollution.

In recent years many researchers have been trying to develop catalysts for the selective conversion of propane to acrylonitrile because of the considerable price difference between propane and propene.^{2–4} However, the selective conversion of propane to acrylonitrile is much more difficult than that of propene due to the low reactivity of propane. All existing commercial processes for the production of acrylonitrile use propene as a feedstock. BP/Sohio Chemicals recently announced an additional production line for direct conversion of propane to acrylonitrile. Thus far, two families of catalysts, Sb^{5–7} and Mo-based catalysts,^{8,9} have been discovered for this purpose. In the case of propene ammoxidation, the Mo-based system is superior to the Sb-based catalysts. Similar to the acrylonitrile case, extensive efforts are being expended to replace the propene-based acrylic acid process with a propane-based process.

We found that a Ca–Bi–Mo oxide catalyst was highly active and selective for ammoxidation of propane to acrylonitrile, and that the performance of the catalyst depended sharply on the

oxide composition.¹⁰ However, the phases present in this oxide system were not known. In light of the importance of this catalyst, the physicochemical properties of the Ca–Bi–Mo oxide were investigated with XRD (powder), XPS, IR/Raman, and TPRX/TPRO to explain the catalytic properties. In addition, this study was intended to correlate the physicochemical properties of catalyst (ability of redox, atomic composition of surface and bulk, kind of phases) with their catalytic performances for propane ammoxidation.

Experimental Section

(a) Catalyst Preparation. The Ca–Bi–Mo oxides with various compositions were reproducibly prepared by a precipitation method including the exact control of experimental parameters such as pH in mixture solution and increasing rate of temperature during calcination.¹⁰ Ammonium molybdate ((NH₄)₆Mo₇O₂₄·4H₂O, Aldrich, 99.98%) was dissolved in a basic ammonia solution (pH 10). This solution was added dropwise to a nitrous solution of bismuth nitrate (Bi(NO₃)₃·5H₂O, Aldrich, 99.99%) and calcium nitrate (Ca(NO₃)₂·4H₂O, Aldrich, 99.99%), and then dilute ammonia was added until the pH of the solution reached 5. After heating at 80 °C with vigorous stirring to evaporate water, a viscous slurry was obtained and subsequently dried at 120 °C for 24 h, precalcined at 320 °C for 3 h in an air stream, and ground. A 100/200 mesh sieve was used to collect powders with sizes between 100 and 200 mesh. Finally, this product was calcined at 520 °C for 6 h in an air stream. The catalysts were pale yellow.

(b) Reaction Procedure. The propane ammoxidation was carried out at atmospheric pressure with a continuous flow reactor system. The reaction products were analyzed by using an on-line gas chromatograph (HP 5890) with two different

* To whom correspondence should be addressed. E-mail: siwoo@kaist.ac.kr. Phone: +82-42-869-3918. Fax: +82-42-869-8890

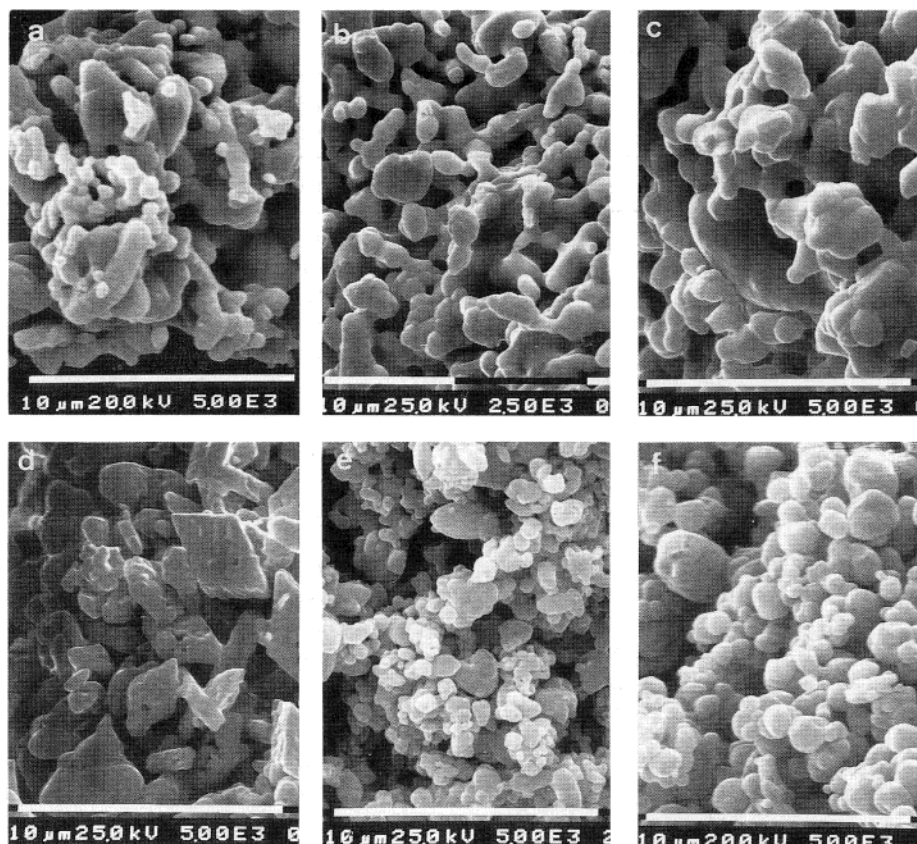


Figure 1. SEM micrograph for $\text{Ca}_x\text{Bi}_{12-x}\text{Mo}_{12}$ oxide: (a) $x = 0$, (b) $x = 3$, (c) $x = 5$, (d) $x = 7$, (e) $x = 9$, and (f) $x = 12$.

sequential GC columns (Gaskuropack-54, 5 m long, and M.S. 5A, 2 m long). The detailed procedures were described elsewhere.¹¹

(c) Methods of Characterization. X-ray powder diffraction patterns were obtained with a Rigaku GF 2035 X-ray diffractometer with Cu K radiation. The IR spectra were recorded with a Bomem infrared spectrophotometer (Michelson-102), using a conventional KBr disk technique. The Raman spectra were collected with a Spectra-Physics argon ion laser (Model 171) for excitation. About 100–200 mg of each bismuth molybdate sample was pressed onto a thin layer of KBr to provide mechanical support. The pressed sample was then mounted onto a sample holder capable of spinning at 2000 rpm to avoid a local heating effect caused by the focused laser beam. X-ray photoelectron spectra were measured with the Leybold, LHS-10. The magnesium anode ($h\nu = 1253.6$ eV) was used for excitation and the X-ray power supply was run at 10 kV and 100 mA. The samples were deposited as a thin layer on double-sided adhesive tape and introduced into the preparation chamber. The samples were outgassed in the preparation chamber of the spectrometer. The pressure in the analysis chamber was maintained at 3×10^{-9} mbar. The spectra of the C 1s, O 1s, Ca 2p, Mo 3d, and Bi 4f levels were recorded. For calibration of the binding energy a small gold film was vapor-deposited on part of the sample. The Au 4f_{7/2} peak (84.0 eV) was used as a reference. To investigate the reactivity of surface oxygen species and redox ability, TPRX/TPRO was carried out. The ammoxidation of propene to acrylonitrile in the absence of gaseous oxygen was performed at a flow rate of 30 cm³/min. The reactant mixture of C₃H₆/NH₃/N₂ (5/5/90%) was passed through the catalyst. The reactor was heated from 298 to 793 K at a rate of 10 deg K/min, held for 30 min, and then cooled to room temperature. During each run, effluent gases were monitored for CO₂ and acrylonitrile to investigate the reactivity

of the surface oxygen species. Reduced oxides were flushed with N₂ at 500 °C for 1 h, and then cooled to room temperature. N₂ was changed with 10% O₂ gas at a flow rate of 30 cm³/min. The reactor was heated from 298 to 793 K at a rate of 10 deg K/min and then cooled to room temperature. The consumption of O₂ arising from the reoxidation of catalysts was monitored by the computer-interfaced mass spectrometer.

Results and Discussion

(a) Effect of the Oxide Composition on the Structure. In our previous research,¹⁰ the selectivity of propane toward acrylonitrile according to the values of x (moles of Ca) in $\text{Ca}_x\text{Bi}_{12-x}\text{Mo}_{12}$ oxide catalysts was reported. The maximum selectivity of propane to acrylonitrile occurred when x was between 6 and 9. For $x > 9$, carbon oxides increased with increasing x . For $x < 6$, propene was the principal product. Because the basicity of the catalyst increased with the increase of x (content of calcium), the oxidation reaction of propene and/or acrylonitrile to carbon oxides was enhanced. The optimum content of Ca for reaction of propane to acrylonitrile was obtained at values of x from 6 to 9. It can be suggested that the difference in catalytic performance depends on the presence of adequate redox and acid–base properties of the catalyst system, because these properties strongly affect the transfer of lattice oxygen and electron between catalyst and reactants. In this paper, the physicochemical properties of Ca–Bi–Mo oxide were investigated with XRD (powder), XPS, IR/Raman, and TPRX/TPRO to explain the catalytic properties of propane ammoxidation. Scanning electron micrographs (SEM) of catalysts with different values of x are shown in Figure 1. Surface morphologies of the catalysts are of variable shape and size depending on the composition of the catalyst. Figure 2 shows the XRD patterns of the Ca–Bi–Mo oxide catalysts according

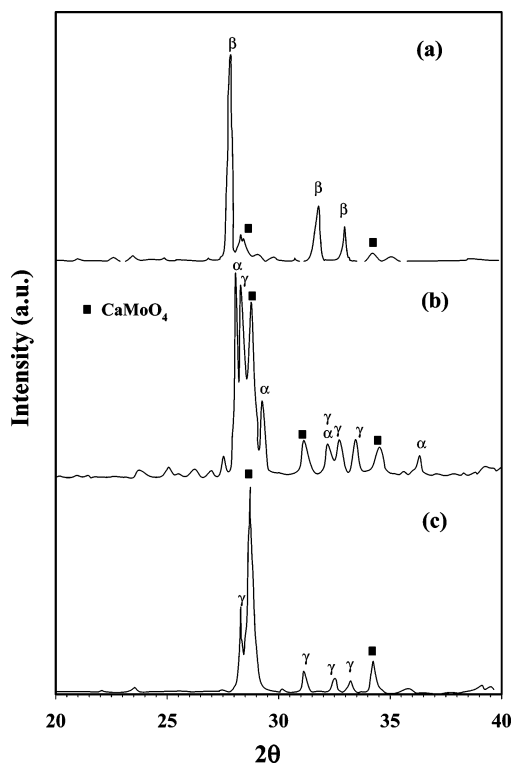


Figure 2. XRD patterns of (a) $\text{Ca}_3\text{Bi}_9\text{Mo}_{12}$ oxide, (b) $\text{Ca}_6\text{Bi}_6\text{Mo}_{12}$ oxide, and (c) $\text{Ca}_9\text{Bi}_3\text{Mo}_{12}$ oxide.

to composition. The phases of the Ca–Bi–Mo oxides varied with the Ca/Bi atomic ratio. $\text{Ca}_3\text{Bi}_9\text{Mo}_{12}$ oxide (Ca/Bi = 1/3) consisted of two phases, β -bismuth molybdate ($\beta\text{-Bi}_2\text{Mo}_2\text{O}_9$) and CaMoO_4 . $\text{Ca}_6\text{Bi}_6\text{Mo}_{12}$ oxide (Ca/Bi = 1/1) consisted of α - and γ -bismuth molybdate ($\alpha\text{-Bi}_2\text{Mo}_3\text{O}_{12}$ and $\gamma\text{-Bi}_2\text{MoO}_6$) and CaMoO_4 . $\text{Ca}_9\text{Bi}_3\text{Mo}_{12}$ oxide (Ca/Bi = 3/1) consisted of γ -bismuth molybdate ($\gamma\text{-Bi}_2\text{MoO}_6$) and CaMoO_4 . Conclusively, the addition of Ca oxide to Bi–Mo oxide caused the formation of different Bi–Mo oxide phases. As mentioned in our previous results¹⁰ the selectivity of propane toward acrylonitrile on $\text{Ca}_6\text{-Bi}_6\text{Mo}_{12}$ and $\text{Ca}_9\text{Bi}_3\text{Mo}_{12}$ oxides was much higher than that of $\text{Ca}_3\text{Bi}_9\text{Mo}_{12}$ oxide. γ -Bismuth molybdate was not contained in $\text{Ca}_3\text{Bi}_9\text{Mo}_{12}$, while it was contained in both $\text{Ca}_6\text{Bi}_6\text{Mo}_{12}$ and $\text{Ca}_9\text{Bi}_3\text{Mo}_{12}$ oxides. Thus γ -bismuth molybdate oxide phase was considered to be a selective phase for propane ammoxidation. To investigate the synergy effect of the phases present in the $\text{Ca}_6\text{Bi}_6\text{Mo}_{12}$ oxide which are composed of α -, γ -bismuth molybdate and CaMoO_4 , the reaction were performed with the physical mixtures of pure corresponding molybdates. The acrylonitrile selectivity (18%) obtained with the mechanical mixture (α - + γ -bismuth molybdate + CaMoO_4) was lower than that of $\text{Ca}_6\text{Bi}_6\text{Mo}_{12}$ oxide catalyst in the propane ammoxidation. This indicated that $\text{Ca}_6\text{Bi}_6\text{Mo}_{12}$ oxide catalyst did not consist of the mixture of pure molybdates (α - + γ -bismuth molybdate + CaMoO_4), but consisted of modified multicomponent oxide phases. Therefore, it can be suggested that the higher selectivity of $\text{Ca}_6\text{Bi}_6\text{Mo}_{12}$ oxide could be attributed to the modified molybdate phases produced by the solid solution reaction, even though the XRD results could not identify this phase.

(b) Formation of Defect Evidenced by IR, XRD, and Raman. The infrared spectra of $\text{Ca}_{1-3x}\text{Bi}_x\text{Mo}_{12}$ oxides are shown in Figure 3. The CaMoO_4 oxide has the ABO_4 scheelite structure (space group C_{4h}) in which all Mo atoms were tetrahedrally coordinated by oxygen at a distance of ca. 1.775 Å.¹² In addition, all oxygen atoms were bridged between Ca

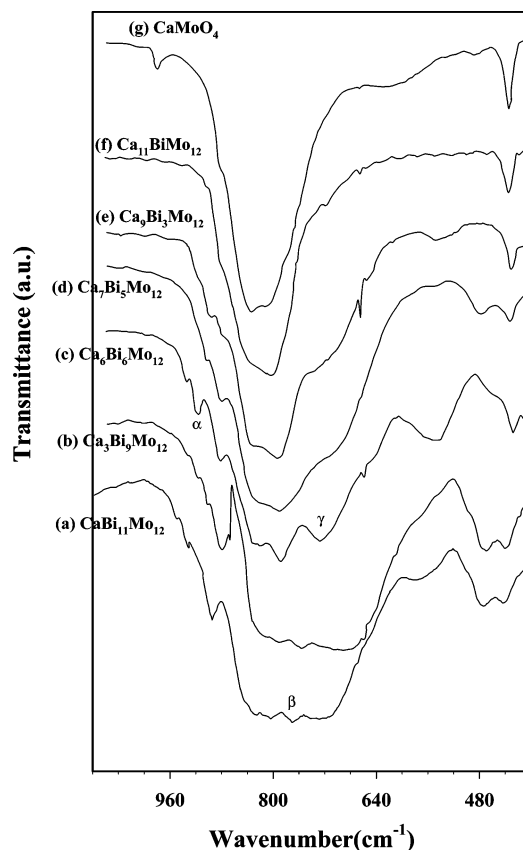


Figure 3. Infrared spectra of Ca–Bi–Mo oxide.

and Mo cations. The IR spectrum of CaMoO_4 oxide (Figure 3g) showed that the characteristic band at 820 cm^{-1} was associated with tetrahedral MoO_4 species. With the addition of bismuth ($x = 1$), the IR spectrum of $\text{Ca}_{11}\text{BiMo}_{12}$ oxide (Figure 3f) is slightly different from that of pure CaMoO_4 . With increasing bismuth concentration of $x = 3$, additional adsorption bands appear at ca. 900 cm^{-1} and ca. 700 cm^{-1} as shown in Figure 3e. The broad band at 720 cm^{-1} can be assigned to the modified γ -bismuth molybdate. The bands at 900 and 890 cm^{-1} are arising from the formation of the higher order Mo–O bond. It was known that the Mo–O bond located next to the cation vacancies has bond orders greater than one.¹³ In the case of Pb–Bi–Na–Mo oxide, the Mo–O stretching band at higher wavenumbers clearly revealed that this band was arising from the cation vacancy and that the intensity of this band was proportional to the concentration of cation vacancy.¹⁴

In the case of $\text{Ca}_6\text{Bi}_6\text{Mo}_{12}$, the IR bands were observed at $930, 895, 840, 800,$ and 730 cm^{-1} . These bands correspond to the characteristic IR bands of CaMoO_4 and α - and γ -bismuth molybdate. The IR spectrum of $\text{Ca}_3\text{Bi}_9\text{Mo}_{12}$ showed broad bands between 650 and 850 cm^{-1} . This oxide is composed of β -bismuth molybdate and CaMoO_4 . These IR results are correlated with the XRD results. It was noteworthy that highly active and selective catalysts were $\text{Ca}_6\text{Bi}_6\text{Mo}_{12}$ and $\text{Ca}_9\text{Bi}_3\text{Mo}_{12}$ oxide having high order Mo–O. In Figure 4, Raman spectra of $\text{Ca}_{1-3x}\text{Bi}_{2x}\text{Mo}_{12}$ oxide are shown as a function of bismuth content (or cation vacancies). The spectrum of CaMoO_4 (at $x = 0$) is in good agreement with previous results.¹² Four bands at $875, 817, 815,$ and 790 cm^{-1} are assigned to Mo–O stretching frequencies. The bismuth (at $x = 0.05$) was added to the CaMoO_4 phase and its new Raman spectra at 920 cm^{-1} was shown in Figure 4b, which is arising from Mo–O bonds located next to cation vacancies. Figure 5 shows the Raman spectra of Ca–Bi–Mo oxides. The Raman spectrum of $\text{Ca}_3\text{Bi}_9\text{Mo}_{12}$ oxide

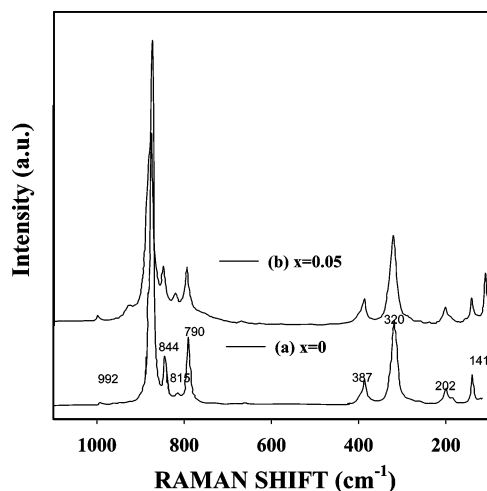


Figure 4. Raman spectra of the $\text{Ca}_{1-3x}\text{Bi}_{2x}\text{MoO}_4$ oxide: (a) $x = 0$ and (b) $x = 0.05$.

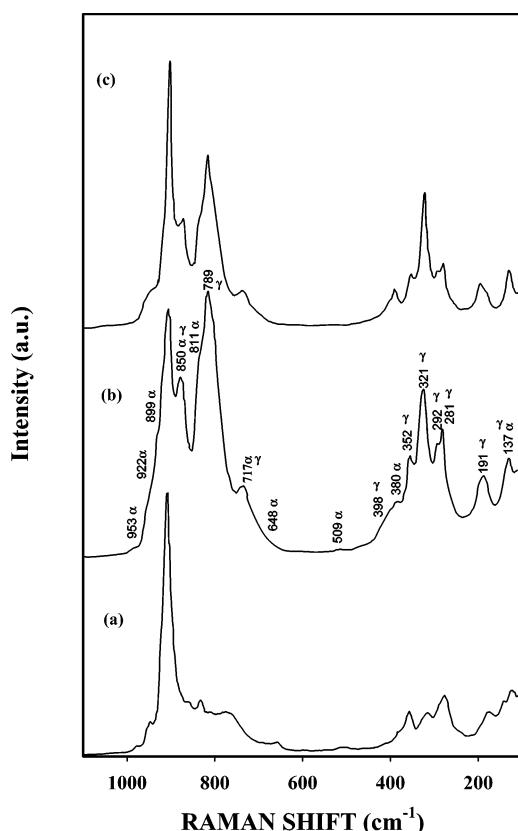


Figure 5. Raman spectra of the (a) $\text{Ca}_3\text{Bi}_9\text{Mo}_{12}$ oxide, (b) $\text{Ca}_6\text{Bi}_6\text{Mo}_{12}$ oxide, and (c) $\text{Ca}_9\text{Bi}_3\text{Mo}_{12}$ oxide.

(Figure 5a) indicates the presence of β -bismuth molybdate and CaMoO_4 , whereas the $\text{Ca}_6\text{Bi}_6\text{Mo}_{12}$ oxide is composed of α -, γ -bismuth molybdate and CaMoO_4 . The Raman spectrum of $\text{Ca}_9\text{Bi}_3\text{Mo}_{12}$ oxide (Figure 5c) indicates the presence of γ -bismuth molybdate and CaMoO_4 .¹⁵ A new band at 920 cm^{-1} was also observed in all of the Ca–Bi–Mo oxides. From these IR and Raman results, it can be concluded that defective Bi–Mo–O oxide having the scheelite structure was produced by adding bismuth oxide to CaMoO_4 oxide.

In the case of CaMoO_4 with the scheelite structure, it is possible to form cation vacancies and the ternary Ca–Bi–Mo phase by the replacement of Ca^{2+} with Bi^{3+} in the CaMoO_4 phase.¹⁶ Although a small number of defects are formed in the bulk, a large number of defects must be present on the surface

TABLE 1: Surface Concentration of Ca–Bi Molybdate Oxide Catalysts

	BiMo	$\text{Ca}_3\text{Bi}_9\text{Mo}_{12}$	$\text{Ca}_6\text{Bi}_6\text{Mo}_{12}$	$\text{Ca}_9\text{Bi}_3\text{Mo}_{12}$	CaMoO_4
O (1s)	57.0	58.4	61.2	59.8	57.7
Mo (3d)	18.7	20.0	21.8	21.4	20.6
Bi (4f)	24.3	18.5	10.3	7.6	
Ca (2p)		2.8	6.7	11.2	20.3

TABLE 2: Atomic Concentration of Ca–Bi Molybdate Oxide after 30 min of Sputtering

	$\text{Ca}_3\text{Bi}_9\text{Mo}_{12}$	$\text{Ca}_6\text{Bi}_6\text{Mo}_{12}$	$\text{Ca}_9\text{Bi}_3\text{Mo}_{12}$
O	57.7	56.8	57.0
Mo	26.3	26.9	27.1
Bi	13.0	6.5	4.8
Ca	3.2	9.8	13.1

because of the tendency of the defect to migrate into the surface and the higher coordinative unsaturated degree of the surface. The catalytic properties are greatly influenced by the small number of defects. The role of the defects must be to stimulate allyl formation and to facilitate the diffusion of the lattice oxygen, resulting in the higher selectivity toward acrylonitrile. In the oxidation of propane to acrolein, the catalytic performance of bismuth vanadomolybdate oxide varied with the concentration of the defect and the highest yield was obtained with the catalyst $\text{Bi}_{0.85}\text{V}_{0.55}\text{Mo}_{0.45}$.¹⁷ In the ammoxidation of propane to acrylonitrile, $\text{Bi}_{0.85}\text{V}_{0.55}\text{Mo}_{0.45}$ oxide catalyst also showed a good catalytic performance. It was thought that there are appropriate cation vacancies in $\text{Bi}_{0.85}\text{V}_{0.55}\text{Mo}_{0.45}$. These cation vacancies generate higher order Mo–O centers, which make lattice oxygen available for the partial oxidation. Also, vacancies improve the mobility of the lattice oxide ions, which in turn enhance the replacement of oxygen ion in the redox cycle of the catalyst.

(c) XPS Study of Ca–Bi–Mo Oxides. The X-ray photoelectron spectra of the Ca–Bi–Mo oxide are shown in Figure 6. The elements Bi, Mo, Ca, and O were detected on the catalyst surface. The elements Mo, Bi, and Ca were assigned to Mo^{6+} , Bi^{3+} , and Ca^{2+} , respectively.^{18,19} The variations of binding energies for these elements were very low in Ca–Bi–Mo oxide. From the Mo 3d spectra of the catalysts, we could ensure that most of the Mo presented as Mo^{6+} in oxidic surroundings. In addition, the broadening of Mo 3d and O 1s spectra was observed, indicating that there were several molybdenum and oxygen species having slightly different binding energy levels on the surface and that the catalyst was modified by adding the bismuth oxide to CaMoO_4 . Tables 1 and 2 showed composition differences between the surface and the bulk, respectively. The mole ratio of elements on the surface depended on components constituting the oxides due to the difference of surface tension of each element. It was clear that the bismuth was mostly observed on the surface of Ca–Bi–Mo oxide. The mole ratio of elements in the bulk was measured after sputtering of Ar^+ ion with the ion energy of 2.5 keV. Bismuth decreased and calcium increased, compared with the results of the surface. It indicated that the concentration of bismuth in the Ca–Bi–Mo oxide decreased from the surface to an inner layer of the catalysts, while the concentration of calcium increased from the surface to an inner layer. Considering that $\text{Ca}_6\text{Bi}_6\text{Mo}_{12}$ and $\text{Ca}_9\text{Bi}_3\text{Mo}_{12}$ were selective for the reaction of propane to acrylonitrile and that an appropriate amount of Ca oxide was also present on the surface of these catalysts along with Bi and Mo oxides in Table 1, it was clear that these catalysts could generate the active site such as defective Ca–Bi–Mo oxide, which had strongly influenced the reaction of propane to acrylonitrile.

(d) Redox Properties. To investigate the reactivity of the surface oxygen species on Ca–Bi–Mo oxide, the ammoxidation

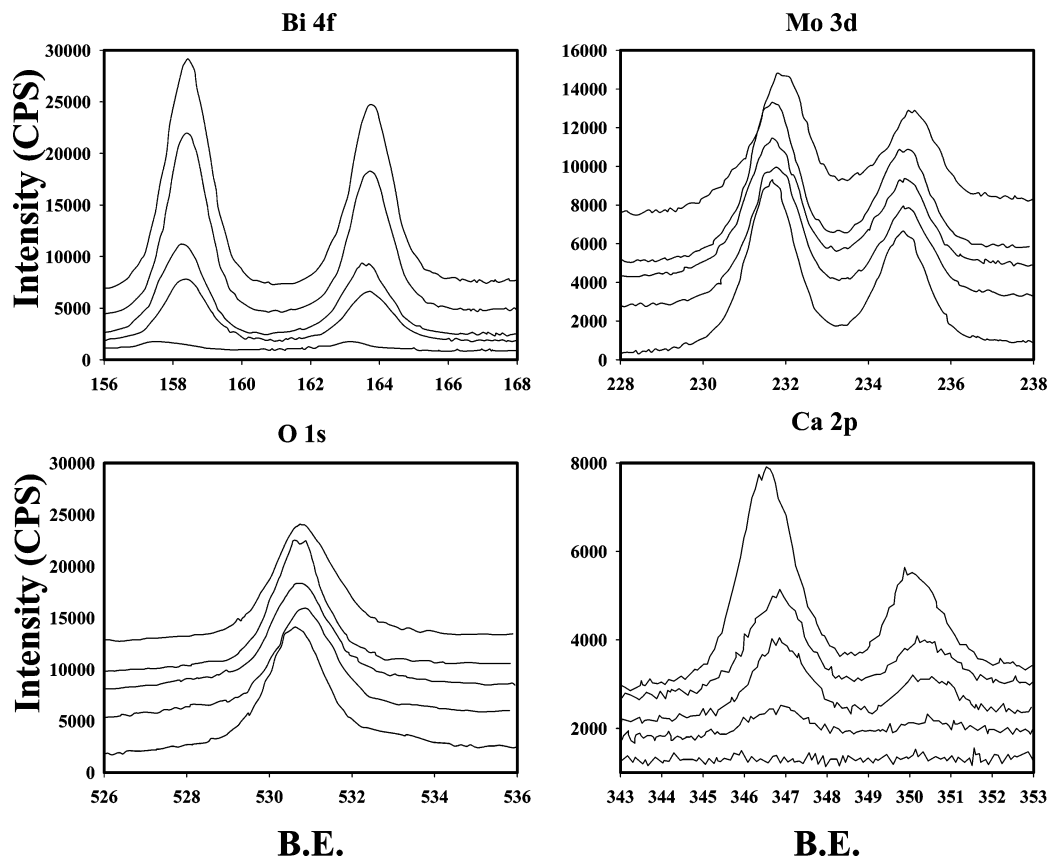


Figure 6. XPS spectra of Bi 4f, Mo 3d, Ca 2p, and O 1s in Ca–Bi–Mo oxide: (a) CaMoO_4 , (b) $\text{Ca}_3\text{Bi}_9\text{Mo}_{12}$ oxide, (c) $\text{Ca}_6\text{Bi}_6\text{Mo}_{12}$ oxide, (d) $\text{Ca}_9\text{Bi}_3\text{Mo}_{12}$ oxide, and (e) BiMo oxide.

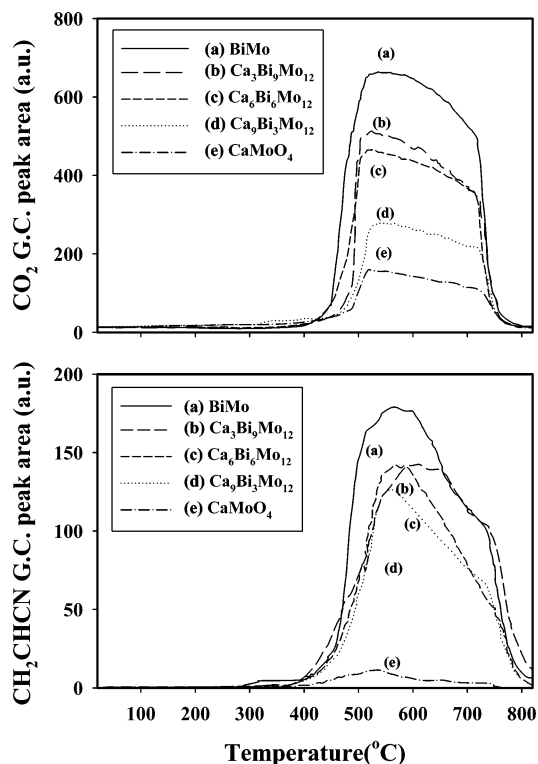


Figure 7. TPRX profile of the Ca–Bi–Mo oxide system.

of propene in the absence of gaseous oxygen was performed. The CO_2 and acrylonitrile in the products were monitored by a quadrupole mass spectrometric analyzer as shown in Figure 7. At the reaction temperature of about 400 °C, the surface oxygen species was initiated with reactants. Comparing the amount of

CO_2 with acrylonitrile, the amount of CO_2 was higher than that of acrylonitrile, indicating that the sites for complete oxidation on the surface were more than those for selective oxidation. In addition, the relative ratio of CO_2 to acrylonitrile depended on the composition of catalysts. In the case of BiMo oxide, the amount of CO_2 was higher than that of the other catalysts. It was supposed that the BiMo oxide had the larger amount of O_2^- or O^- species than other catalysts, in that the O^- or O_2^- species were strongly electrophilic reactants which are responsible for the complete oxidation.²⁰ In the case of olefins, this electrophilic addition of O_2^- or O^- results in the formation of peroxy or epoxy complexes, respectively which were the intermediates of the degradation of the carbon skeleton and total oxidation in the conditions of heterogeneous catalytic oxidation.²¹ When the content of calcium oxide gradually increased, the amount of CO_2 rapidly decreased, while acrylonitrile was nearly constant. It indicated that the active sites of complete oxidation on the surface were diminished by addition of calcium oxide. The reduced state of the catalysts was investigated by using the TPRO technique. The TPRO profiles of the Ca–Bi–Mo oxides were obtained and shown in Figure 8. Two peaks at about 230 and 450 °C were observed for all catalysts except CaMoO_4 , indicating that the reduced Ca–Bi–Mo oxides might be reoxidized in these two temperatures. In the case of CaMoO_4 oxide, only one peak was observed at 420 °C and the consumption of gaseous oxygen was the smallest in the Ca–Bi–Mo oxides, indicating that the CaMoO_4 oxide had a small ability to redox cycle. The first peak in TPRO profiles came from the reoxidation of the reduced bismuth. Miura et al. reported that the reoxidation of reduced bismuth oxide (25% at 400 °C) took place at 230 °C.²² The reduction of bismuth oxide should produce metallic bismuth only. The second reoxidation step suggested by the peak at 450 °C may be the reoxidation of

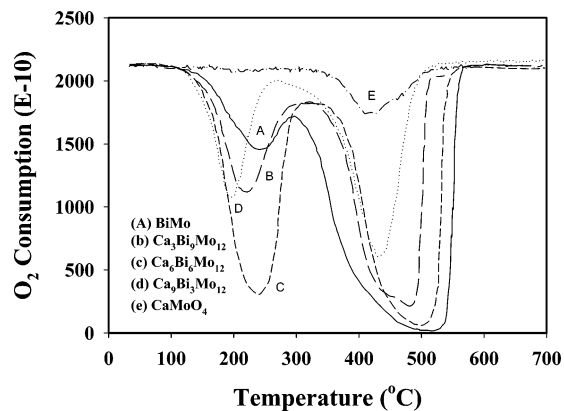


Figure 8. TPRO profile of the Ca–Bi–Mo oxide system.

molybdenum oxide. When bismuth oxide was added to CaMoO_4 , the ability for reoxidation increased with the addition of bismuth oxide. In particular, the increase of reoxidation at the second peak was explained by cation vacancies of the Ca–Bi–Mo oxide as mentioned in previous IR and Raman results. When calcium oxide was added to BiMo oxide, the ability for reoxidation at the first peak was greatly enhanced. It was thought that the bismuth ions on the surface might act as the sites for the adsorption of gaseous oxygen and the oxidation state of bismuth would probably be the highest, i.e., Bi(V).

Conclusions

The physicochemical properties of highly active and selective Ca–Bi–Mo oxide for ammoxidation of propane to acrylonitrile were investigated by powder XRD, IR/Raman, XPS, and TPRX/TPRO (temperature programmed reaction/temperature programmed reoxidation) techniques. The phases in the Ca–Bi–Mo oxide varied with the composition of the oxide. The γ -bismuth molybdate ($\gamma\text{-Bi}_2\text{MoO}_6$) in both $\text{Ca}_6\text{Bi}_6\text{Mo}_{12}$ oxide and $\text{Ca}_9\text{Bi}_3\text{Mo}_{12}$ oxide is considered to be the active phase for propane ammoxidation to acrylonitrile. The defective Ca–Bi–Mo oxide produced by the addition of Bi oxide played an important role in propane ammoxidation. The addition of calcium oxide into Bi–Mo oxide decreased the number of active sites for complete oxidation and increased the ability for

reoxidation (O_2 consumption) of reduced catalysts. The catalysts were highly active and selective when an appropriate amount of Ca oxide was present on the surface along with Bi and Mo oxides.

Acknowledgment. This research was funded by Tong-Suh Petrochemical company and CUPS (Center for Ultra-microchemical Process Systems) sponsored by KOSEF (2003-2004). The authors thank Professor I. Wachs and Dr. D. S. Kim for their help in obtaining the Raman spectra.

References and Notes

- (1) Centi, G.; Trifiro, F.; Ebner, J. R.; Franchetti, V. M. *Chem. Rev.* **1988**, *88*, 55.
- (2) Kim, Y. C.; Ueda, W.; Moro-oka, Y. *Appl. Catal.* **1991**, *70*, 189.
- (3) Glaeser, L. C.; Brazidil, J. F.; Toft, M. A. U.S. patent, 5 097 207, 1992.
- (4) Seely, M. J.; Friedrich, M. S.; Suresh, D. D. U.S. patent, 4 978 764, 1990.
- (5) Guerrero-Pérez, M. O.; Fierro, J. L. G.; Banares, M. A. *Catal. Today* **2003**, *78*, 387.
- (6) Nguyen, D. L.; Taarit, Y. B.; Millet, J.-M. M. *Catal. Lett.* **2003**, *90*, 65.
- (7) Zanthoff, H. W.; Grunert, W.; Buchholz, S.; Heber, M.; Stievano L.; Wagner, F. E.; Wolf, G. U. *J. Mol. Catal. A: Chem.* **2000**, *162*, 443.
- (8) Holmberg, J.; Grasselli, R. K.; Andersson, A. *Top. Catal.* **2003**, *23* (1–4), 55.
- (9) Asakura, K.; Nakatani, K.; Kubota, T.; Iwasawa, Y. *J. Catal.* **2000**, *194* (2), 309.
- (10) Kim, J. S.; Woo, S. I. *Appl. Catal.* **1994**, *110*, 173.
- (11) Kim, J. S.; Woo, S. I. *Appl. Catal.* **1994**, *110*, 207.
- (12) Hardcastle, F. D.; Wachs, I. E. *J. Phys. Chem.* **1991**, *95*, 26.
- (13) Brazidil, J. F.; Glaeser, L. C.; Grasselli, R. K. *J. Catal.* **1983**, *81*, 142.
- (14) Aykan, K.; Sleight, A. W.; Rogers, B. *J. Catal.* **1973**, *31*, 185.
- (15) Hardcastle, F. D.; Wachs, I. E. *J. Raman Spectrosc.* **1990**, *25*, 683.
- (16) Sleight, A. W.; Aykan, K.; Rogers, D. B. *J. Solid State Chem.* **1975**, *13*, 231.
- (17) Kim, Y. C.; Ueda, W.; Moro-oka, Y. *Appl. Catal.* **1991**, *70*, 175.
- (18) Mitsuura, I.; Walfs, M. W. J. *J. Catal.* **1975**, *37*, 174.
- (19) Wagner, C. D.; Riggs, W. M.; Davis, L. E.; Moulder, J. F.; Muilenberg, G. F. *Handbook of X-ray Photoelectron Spectroscopy*; Perkin-Elmer: Eden Prairie, MN, 1978.
- (20) Keulks, G. W.; Liao, N.; An, W.; Li, D. *Int. Congr. Catal., 10th, Budapest, Hungary* **1993**, 2253.
- (21) Haber, J. In *Surface properties and Catalysis by Nonmetals*; Bonnelle, J. P., Delmon, B., Derouane, E., Eds.; D. Reidel Publishing Co.: Dordrecht, The Netherlands, 1982; 1.
- (22) Miura, H.; Morikawa, Y.; Shirasaki, T. *J. Catal.* **1975**, *39*, 22.